Proceedings of the 39th Chinese Control Conference
July 27-29, 2020, Shenyang, China

Balance Control of a Wheeled Hopping Robot

Lufeng Zhang[1], Xuemei Ren[1], Qing Guo[2]

1. School of Automation, Beijing Institute of Technology, Beijing 100081, China
E-mail: zlf2018@163.com , E-mail: xmren@bit.edu.cn

2. School of Computer Science and Technology, Beijing Institute of Technology, Beijing 100081, China
Email: glorygq@163.com

Abstract: The objective of this paper is to control a wheeled hopping robot. The balance of the wheeled hopping robot is so important whether in the forward mode or hopping mode. In this paper, we firstly introduced our designed wheeled hopping robot including the mechanical design and the drive components. A set of gear transmission system and cable structure are used for the forward mode and the hopping mode switch. Differing from the traditional inverted pendulum model, the dynamical model of this wheeled hopping robot is changing due to the torsional spring, so the equivalent length of the model is not a constant. Meanwhile, the elastic element made the robot less stable than an inverted two-wheel robot. We adopted different closed-loop control algorithms to solve the problems in upright, speed and turning control. Finally, the experimental results were shown in this paper.

Key Words: Wheeled hopping robot, Balance control, Closed-loop control, Experiment result.

1 Introduction

Researchers around the world have been studying various robots for exploration in extreme environment. Like the origami wheeled robot developed by the college using the origami mechanism [1] (see Fig. 1 (a)), the sections of the robot's wheel structure are connected to each other by folding, which provides the transmission of maintaining geometry and force. The wheel diameter varies from 4cm to 11cm, and it is tightened or released by 4 SMA coil springs to achieve the wheel diameter change. The disadvantage of the special-shaped wheel robot based on the origami mechanism is that the wheel diameter can be changed but the strength is small due to the use of folds on the wheel. In addition, although the change of the wheel diameter is controllable, it needs an additional motor to achieve it, increasing the complexity of the structure.

The more common structure for robots that use special-shaped wheels to overcome obstacles is, for example, the Whegs robot [2] (see Fig. 1 (b)) designed by Case Western Reserve University in the United States. Its main principle is that of bionic insect legs. The miniature contact foot changes the round wheel into a leg-type wheel, which increases the adhesion between the wheel and the obstacle to overcome obstacles. This special-shaped wheel can, to some extent, have a higher obstacle clearance ability than a round gear of the same size, but its main disadvantages are that the size of the wheels cannot be changed, and the ability to overcome obstacles is limited. At the same time, when traveling on a flat road, the overall movement of the car body is not stable due to the moment of change of the center of gravity of the wheels. Similarly, on the basis of the contact leg wheels, Virginia Tech controls each contact leg on the wheel with a motor and gear structure to achieve the free expansion and contraction of each contact leg. The robot is shown in [3], its flexibility and stability are stronger, but it also brings the complexity of the control system and the increase in overall size.

Beijing University of Posts and Telecommunications have designed a mobile robot with variable wheel diameter based on the butterfly zoom mechanism theory, which mainly relies on the butterfly zoom wheels shown in Fig. 1 (c) from [4], which can be changed according to the environment. The size of the wheel diameter meets the requirements of complex terrain and the ability to withstand a certain load. It is widely used in life (such as a movable curtain on the stage). The butterfly zoom mechanism is used for wheel design, and can adapt to different heights to a certain extent. Obstacles, likewise, the wheels of this butterfly zoom mechanism have discrete contact points with the ground during operation. Compared with ordinary wheeled wheels, their movements are somewhat unstable.

The water jumping robot [5] jointly developed by the Department of Industrial and Manufacturing Engineering of the University of Hong Kong is shown in Fig. 1 (d). Jumping from the water surface is more difficult than jumping from the ground. To solve this problem, developers use carbon fiber strips to Energy storage, two wings slap on the water surface, a hollow body structure to support the water surface, and intermittent gear mechanism to achieve energy storage and release. The robot finally has only 12.5g, the maximum size is 10cm, and the height of jumping from the water surface is up to 9.5cm, the purpose of this robot was mainly used by the researchers to carry various sensors to detect the water surface environment. Bouncing robots using similar hydraulic or pneumatic drive systems are also quadruped robots developed by the Italian Institute of Technology's Robotics Laboratory [6], Carnegie Mellon University's single-leg bouncing robots [7], and MIT Cheetah Robot [8]. Pneumatic and hydraulic drives are similar, which has the advantage of high power density, suitable for linear motion (output by hydraulic cylinder / pneumatic cylinder), can achieve long-distance driving, and low efficiency if used in rotary motion (hydraulic motor output). In contrast, motor drive is suitable for turning

This work is supported by National Natural Science Foundation (NNSF) of China under Grant 61973036, 61433003.

places. If you want to convert to linear motion, the screw is generally used. This is slower, lower power, higher noise, and requires sealing compared with pneumatic and hydraulic High is a major disadvantage of pneumatic and hydraulic drives.

In this paper, the main objective is to keep the wheeled robot balance when it moves forward and turns. The mechanism of the wheeled hopping robot is introduced. And we will experimentally verify the closed-loop control algorithms. Finally, the future work will be outlined.

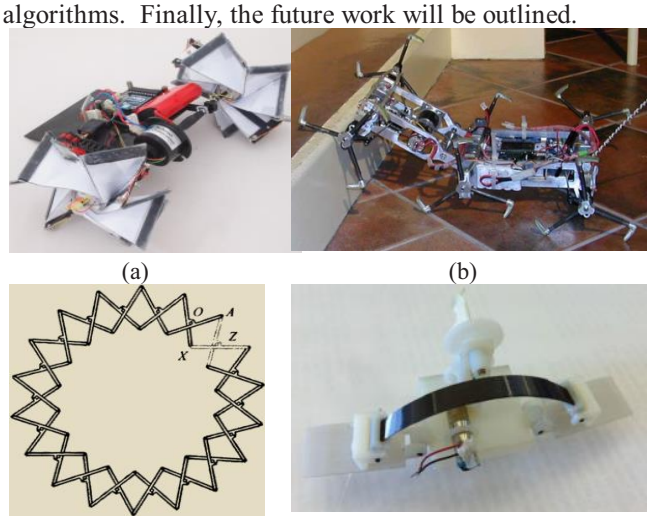

(a) (b) (c) (d)

Fig. 1: Different Robots for Crossing Obstacles

2 Mechanical Design

Hopping motion analysis and the mechanical design is introduced in this section. Through the model simplification, the motion process and controller loop of the wheeled hopping robot can be clearly shown and designed.

The mechanism and driven unit of the wheeled hopping robot is shown in Fig. 2 and Fig. 3. Since the designed self-balancing wheeled hopping robot requires a motor-driven gear train to tighten the fishing line to store the torsion spring energy, the DC motor selected is shown in Fig. 3 (a). Its rated voltage is 12v and the stall torque is 16kg · cm, no-load speed is 100 rpm / min, and reduction ratio is 1: 100.

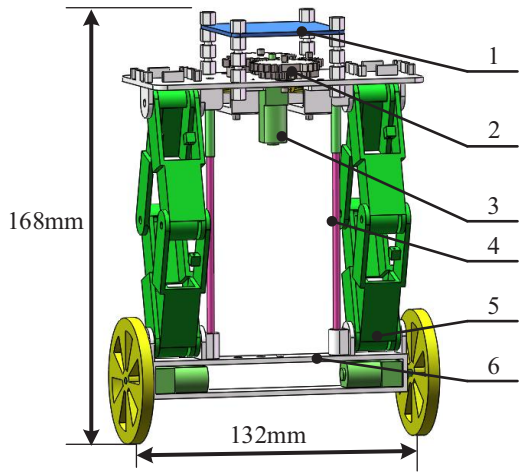

Fig. 2: CAD model of the two-wheel and hopping robot: 1-Control panel 2-Gear train 3-DC motor
4-Guide bar 5-Four-bar linkage 6-Wheel frame

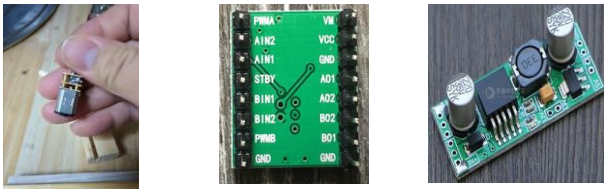

(1) (2) (3)

Fig. 3: Driven components: (1) DC motor (2) Motor driver (3) Voltage stabilizer

Based on our previous work [9], the dynamic model of the robot can be written as follows:

$$\begin{bmatrix} A_{11} & A_{12} \\ A_{21} & A_{22} \end{bmatrix} \begin{bmatrix} \ddot{\theta}_1 \\ \ddot{\theta}_2 \end{bmatrix} + \begin{bmatrix} B_{11} & B_{12} \\ B_{21} & B_{22} \end{bmatrix} \begin{bmatrix} \theta_1 \\ \theta_2 \end{bmatrix} = \begin{bmatrix} \tau_1 \\ \tau_2 \end{bmatrix}$$

It can be seen from the equation above that there is coupling relationship between θ_1 and θ_2, meanwhile, $\tau_1 + \tau_2 = 0$. The coefficient matrix is related to the mass, length and other parameters (as shown in Table 1). The meaning of each parameter in Table 1 was explained in [9]. Obviously, the robot is an underactuated system with elastic element. In this paper, we did the experiments with trial and error based on our experience.

Table 1: Parameters of the Robot Model

Parameters	Value	Parameters	Value
R/mm	25	L/mm	50
h/mm	15.26	s/mm	41.38
d/mm	30	r/mm	6
b/mm	20	e/mm	14
m_w/g	46	$m_i\,(i=1,2,3,4)$/g	7.5
m_u/g	64	Total Weight/g	170
$\rho / kg \cdot m^{-3}$	1.3	A / m^2	0.075
Cd	1.3	$\Delta\theta$	120

3 Closed-loop Control System

In this section, the closed-loop control system is introduced. As mentioned above, when the wheeled hopping robot is moving forward, the balance is an important issue to solve. The tilt angle and the velocity of the wheeled hopping robot should both be feedback signals in the closed-loop control system.

The design of the bouncing wheeled robot of the "inverted pendulum" model used in this paper requires the attitude angle of the robot during the movement of the robot through the gyro sensor [10] [11]. Divided into Kalman

filtering and complementary filtering. As shown in Fig. 3, the left and right diagrams are not in equilibrium, and they tend to fall due to the torque generated by their own gravity. Next, first compare the differences between the two filtering methods, Kalman and complementary filtering, and the control method of wheeled bouncing robot is introduced.

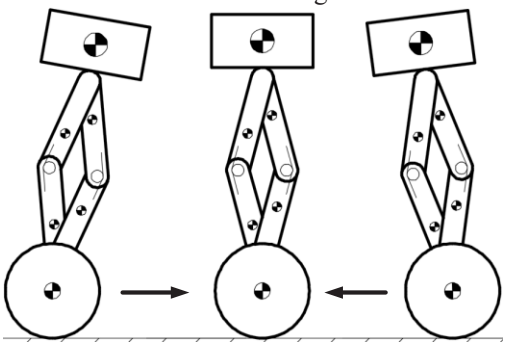

Fig. 3: Schematic diagram of upright control for the wheeled hopping robot

The balance control of this wheeled bouncing robot mainly includes three aspects of control: upright ring control, speed ring control and turning ring control. The specific control schemes for these three aspects are as follows:

(1) *Upright closed-loop control:* During the upright process of the balanced robot, due to the gravity of the robot, the robot is subject to the torque centered on the center of gravity of the robot during the upright process, which will cause the robot to fall. Only when the robot and Y The robot can stay upright only when the included angle of the axis is the value of the included angle when it is balanced.

Here, the PD control algorithm is used to adjust the upright state of the cart with the angle between the cart and the Y axis as negative feedback. The system control block diagram is shown below:

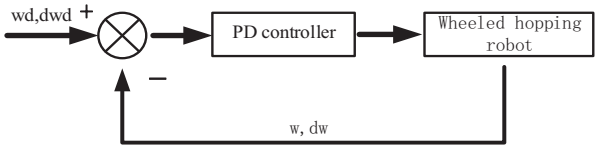

Fig. 4: Block diagram of vertical ring control for the wheeled hopping robot

Among them, the PD controller uses the PD algorithm and the proportional link to enhance its response speed and control its overshoot, and the differential link to suppress its oscillation and quickly reach a balanced and stable state. The set value here is the angle between the body and the Y axis when the robot is balanced. The feedback value is the angle between the robot body and the Y axis measured in real time during the robot's operation. The output of the upright PD controller is used as the voltage input required to control the operation of the robot. During the running of the program, the input control voltage of the balancing robot is continuously adjusted by the difference between the set value and the actual measured value, and then the movement state of the body is changed, so as to adjust the angle between the robot body and the Y axis until the actual When the measured value is equal to the initial measured value, the robot can remain upright. At this time, the output voltage of the controller is zero, and the robot's motion status is unchanged, and it will always be in equilibrium.

(2) *Speed loop control:* In the process of speed loop tuning, the balancing robot must first ensure the upright state of the body, and then ensure the robot's running speed. Here we need to use cascade PID [12] control. In order to ensure that the upright ring of the balancing robot has absolute priority, the output of the upright ring regulator is directly used as the input of the balancing robot. Then add a speed controller in front of the upright ring controller to control the speed. The control block diagram is as follows:

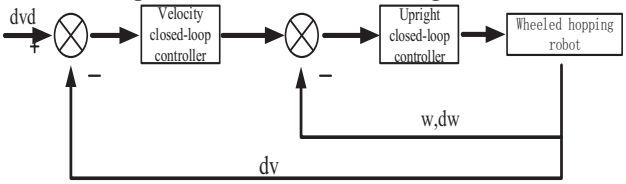

Fig. 5: Speed loop control block diagram for the wheeled hopping robot

The feedback in the control system has two values, which are angle and speed. The angle feedback is to keep the balancing robot in a balanced state at all times, and the speed feedback is to control the running speed of the robot to maintain a stable value. Because the angle between the balance robot and the Y axis is different at different running speeds, the output value of the speed loop can be input to the upright controller as the initial value of the angle of the upright closed-loop controller.

(3) *Turning control:* In the process of controlling the steering of the robot, it is necessary to ensure that the robot's upright ring control and speed ring control are turned on, and then control the difference between the left and right wheels of the car to perform the robot's steering control. The block diagram of its control system is as follows:

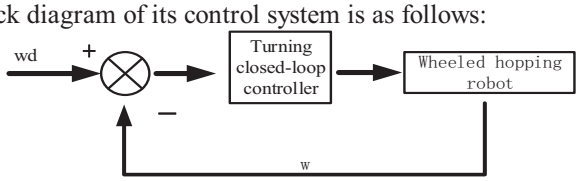

Fig. 6: Turning loop control block diagram of the wheeled hopping robot

The input of this control system is the Z-axis gyroscope value we expect when the robot turns. During the control system operation, the angle integration of the Z-axis gyroscope in real-time feedback is used as negative feedback to adjust the operating status of the entire system. Until the turning angle reaches our preset angle, the output value of the turning closed-loop controller is 0, the adjustment is stopped, and the turning movement is completed.

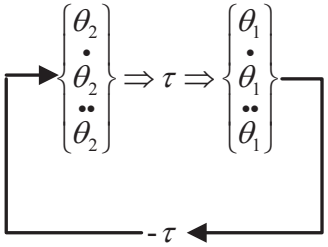

Fig. 7: The Coupling Relationship

4 Experimental Results

After the experimental prototype is completed, the bouncing wheeled robot is subjected to motion experiments

on a flat ground, including experiments on straight travel and turning, to verify the smooth performance of the robot under the PID control algorithm in order to perform the bouncing verification experiment smoothly.

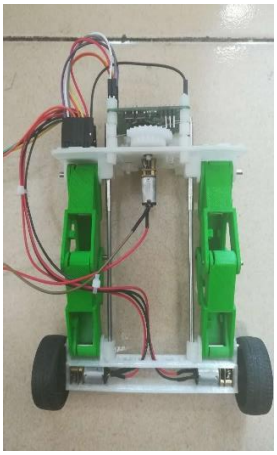

Fig. 8: Porotype of the wheeled hopping robot

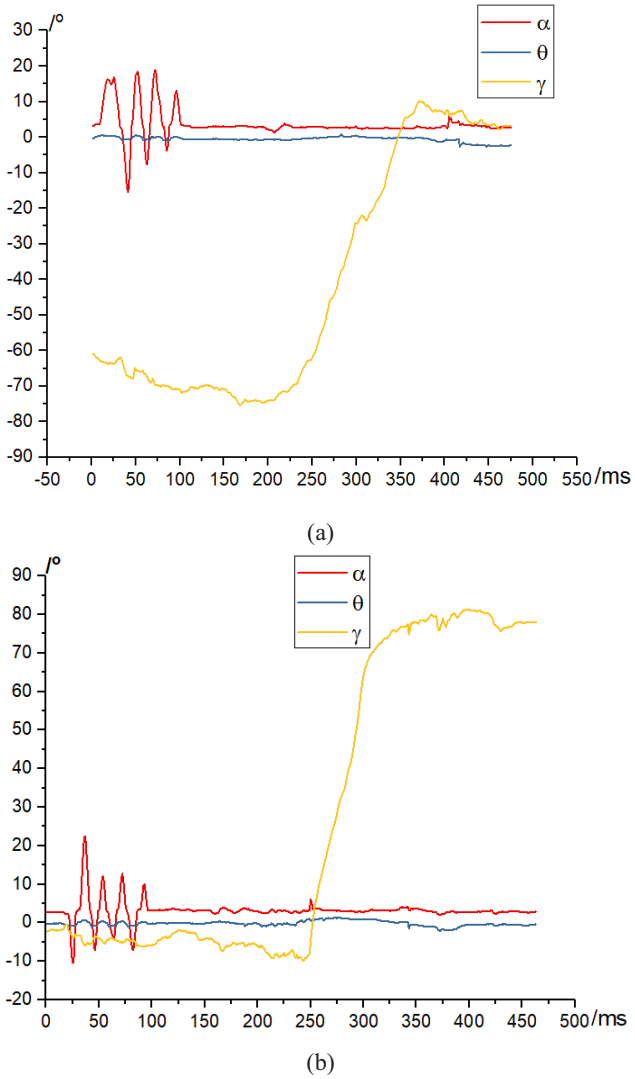

Fig. 9: Real-time motion graph of the wheeled hopping robot along straight line and turning experiment

Figure 9 shows the experimental scenario of this wheeled bouncing robot during straight travel and turning. Figure 8 shows the real-time turning angle change curve during this process. Take the initial movement direction of the robot as the Y axis, the direction perpendicular to the Y axis on the ground is the X axis, and the vertical direction is the Z axis to establish a spatial coordinate system, then α is the angle of the plane where the controller is rotated around the X axis direction, and Θ is the control The rotation angle of the plane where the controller is located around the Y axis. Γ is the rotation angle of the plane where the controller is located around the Z axis. As seen from the change curve of α, the upper and lower jitter ranges in the initial stage are large (between +200 and -150). The initial stage is in the process of balance adjustment. As the robot gradually stabilizes, the curve changes gradually (the change range is less than 50). The change curve of γ reflects the turning process of the robot. In the time period of 200ms ~ 400ms, the change range of γ Close to 900, the robot made a turn during this period of time; during the whole movement, the cymbals were almost unchanged (the amplitude of change was less than 20), indicating that the robot did not turn left and right before turning, and did not tilt forward and backward after turning, and the robot had stable performance.

Fig . 9 (a) and (b) reflect the real-time turning angle changes of the robot's two straight-line traveling and turning experiments, and the observation curve changes. The general trend is the same, but there are also differences. The main difference is that The yellow curve, that is, the change of the rotation angle γ of the robot around the Z axis. The yellow curve in Figure 9 (a) gradually decreases when it starts to travel, indicating that the robot gradually deviates from the original driving direction, and the offset angle is 150. Within, the yellow curve in Figure 9 (b) appears to be more stable. The change in the angle of rotation during the straight forward movement is within 50. The difference occurs when the wheel is removed and fixed. , So that the left and right wheels are better matched in the installation mode and are close to symmetrical, but from the experimental results, it can be found that the deflection still exists in the figure (b), which shows that even if the left and right sides of the robot are structurally symmetrical, they are practically symmetrical. There are other reasons in life that affect the straight line, such as the impact of friction and the real-time response of the motor to commands and programs. This also complements better control strategies. There are demands to compensate for these differences. The changes in the red and green curves in Figure 9 (a) and Figure 9 (b) are not significant, and the smooth conditions reflected are as described above, and both perform well.

5 Conclusion

A novel two-wheel hopping robot is presented in this paper. The balance of the wheeled hopping robot is so important whether in the forward mode or hopping mode. Differing from the traditional inverted pendulum model, the dynamical model of this wheeled hopping robot is changing due to the torsional spring, so the equivalent length of the model is not a constant. Meanwhile, the elastic element made the robot less stable than an inverted two-wheel robot. We adopted different closed-loop control algorithms to solve the problems in upright, speed and turning control. Finally, the experimental results were shown in this paper. The experimental results have good performance while the

wheeled robot is moving forward or turning, and the future work includes the controller design for balance when the robot flights in the air and lands on the road.

References

[1] Lee, Dae Young, et al. Deformable wheel robot based on origami structure [A]. *IEEE International Conference on Robotics and Automation* [C], IEEE, 2013:5612-5617.

[2] Lewinger, William A, et al. Insect-like Antennal Sensing for Climbing and Tunneling Behavior in a Biologically-inspired Mobile Robot [A]. *IEEE International Conference on Robotics and Automation* [C], IEEE, 2005:4176-4181.

[3] Jeans, J. Blake, and D. Hong. IMPASS: intelligent mobility platform with active spoke system [A]. *IEEE International Conference on Robotics and Automation* [C], IEEE, 2009:1605-1606.

[4] 张振华,李端玲. 基于蝶形机构的放缩机构的设计及仿真 [J]. 机电产品开发与创新, 2009, 22.6:38-39.

[5] Jiang, Fei, et al. A Miniature Water Surface Jumping Robot [J]. *IEEE Robotics & Automation Letters*, 2017, 2.3:1272-1279.

[6] Boaventura, T, et al. Dynamic torque control of a hydraulic quadruped robot [A]. *IEEE International Conference on Robotics and Automation* [C], IEEE, 2012:1889-1894.

[7] M. H. Raibert, H. B. Brown, and M. Chepponis, Experiments in balance with a 3D one-legged hopping machine [J], *Int. J. Rob. Res*., 1984, vol. 3, no. 2, pp. 75–92.

[8] Dong, Jin Hyun, et al. High speed trot-running: Implementation of a hierarchical controller using proprioceptive impedance control on the MIT Cheetah [J]. *International Journal of Robotics Research*, 2014, 33.11:1417-1445.

[9] Yanheng Zhang, et al. Design and Implementation of a Two-Wheel and Hopping Robot With a Linkage Mechanism. *IEEE Access. 6*: 42422-42430 (2018)

[10] 魏乐乐. 独轮自平衡车控制系统的开发 [D]. 浙江，杭州. 浙江大学, 2016.

[11] 谭俊杰. 自平衡式两轮电动车电机驱动系统设计 [D]. 辽宁，大连. 大连理工大学, 2015.

[12] Carl F. Schaefer, Kira Anthony, Shiva Krupa, et al. PID: The Pathway Interaction Database [J]. *Nucleic acids research*, 2009, 37 (Database issue):674-9.